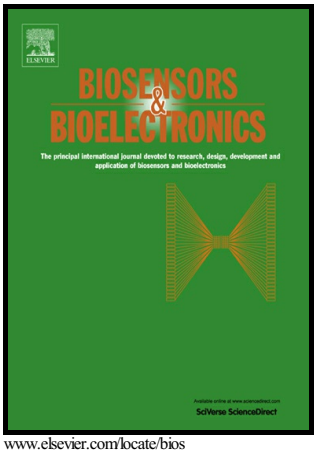

www.elsevier.com/locate/bios

Novel MWCNTs/Graphene Oxide/ Pyrogallol Composite with Enhanced Sensitivity for Biosensing Applications

Mona A. Mohamed, Ali M. Yehia, Craig E. Banks, Nageh K. Allam

PII: S0956-5663(16)31022-3
DOI: http://dx.doi.org/10.1016/j.bios.2016.10.025
Reference: BIOS9247

To appear in: *Biosensors and Bioelectronic*

Received date: 5 September 2016
Revised date: 1 October 2016
Accepted date: 8 October 2016

Cite this article as: Mona A. Mohamed, Ali M. Yehia, Craig E. Banks and Nageh K. Allam, Novel MWCNTs/Graphene Oxide/ Pyrogallol Composite with Enhanced Sensitivity for Biosensing Applications, *Biosensors and Bioelectronic* http://dx.doi.org/10.1016/j.bios.2016.10.025

Novel MWCNTs/Graphene Oxide/ Pyrogallol Composite with Enhanced Sensitivity for Biosensing Applications

Mona A. Mohamed,[1] Ali M. Yehia,[2] Craig E. Banks [3] and Nageh K. Allam[4,*]

[1]Pharmaceutical Chemistry Department, National Organization for Drug Control and Research, Giza, Egypt.

[2]Analytical Chemistry Department, Faculty of Pharmacy, Cairo University, Cairo, Egypt.

[3]Faculty of Science and Engineering, Manchester Metropolitan University, Chester Street, Manchester M1 5GD, UK.

[4]Energy Materials Laboratory, School of Sciences and Engineering, The American University in Cairo, New Cairo 11835, Egypt.

*nageh.allam@aucegypt.edu

Abstract

A novel and highly sensitive biosensor employing graphene oxide nano-sheets (GO), multiwalled carbon nanotubes (MWCNTs), and pyrogallol (PG) was fabricated and utilized for the sensitive determination of omeprazole (OME). The morphological and structural features of the composite material were characterized using different techniques. The modified electrode showed a remarkable improvement in the anodic oxidation activity of OME due to the enhancement in the current response compared to the bare carbon paste electrode (CPE). Sensor composition and measurement conditions were optimized using an experimental design. Differential pulse voltammetry (DPVs) exhibited two expanded linear dynamic ranges of 2.0×10^{-10}–6.0×10^{-6} M and 6.0×10^{-6} – 1.0×10^{-4} M for OME at pH 7 with a detection limit of 1.02×10^{-11} M. The practical analytical utilities of the modified electrode were demonstrated by the accurate determination of OME in pharmaceutical formulation and human serum samples with mean recoveries of 100.97% and 98.58%, respectively. The results clearly revealed that the proposed sensor is applicable to clinical analysis, quality control and routine determination of drugs in pharmaceutical formulations.

Keywords: Omeprazole; graphene oxide; MWCNTs; pyrogallol; biosensor

1. Introduction

Among the most considerable substituted benzimidazole sulfoxides is omeprazole (OME; 5-methoxy-2[[(4-methoxy-3,5-dimethyl-2-pyri-dinyl) methyl] sulphinyl]-1Hbenzidimazole, Scheme 1) that functions as a proton pump inhibitor in

the treatment of gastric ulcers (Olbe et al. 2003). OME has been determined alone or in mixture with other drugs using several techniques (Bosch et al. 2007) and electrochemical methods (Bojdi et al. 2015; El-Enany et al. 2008; Gupta and Goyal 2014; Jorge et al. 2010; Karolia et al. 2015; McClean et al. 1994; Oezaltin and Temizer 1994; Qaisi et al. 2006; Radi 2003).

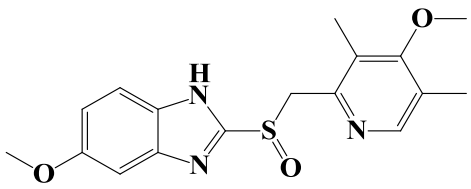

Scheme 1. Chemical structure of OME

In attempt to further enhance the electroanalytical potential of the OME configuration, modification of the graphite working electrode through the introduction of other materials was considered. In latest years, there has been an increasing interest in carbon nanotubes (CNTs), which promote effective electronic transfer, and are extensively used in electroanalytical chemistry (Banks et al. 2005). Those unique properties of CNTs can be related to their high surface area, low over-voltage, and improved electrode kinetics, resulting in low detection limits, high sensitivities and fast responses. Consequent, CNTs have been prognosticated and explored as the most popular nanomaterial for the modification of the electrodes in the electro-analysis of biomolecules (Gao et al. 2012; Mohamed et al. 2016). Specifically, the multi-wall carbon nanotubes (MWCNTs) were thought to have much higher stability against electro-migration than other small metallic structures, recommending their use as possible links in future nano-electronic devices. An important derivative of graphene is graphene oxide (GO), which has a similarly good performance to graphene owing to its high adsorption capacity, large surface area and good biocompatibility. In particular, GO contains a large number of hydrophilic functional groups, such as -OH, -COOH and epoxides on the basal plane and the edge (Stankovich et al. 2007), resulting in good hydrophilicity that makes it easily dispersed in solvents with long-term stability. Based on these advantages, GO-based electrochemical sensors have been developed for the sensitive determination of various biological molecules (Wang et al. 2009). However, pristine GO exhibited weak catalytic performance in some cases due to its poor conductivity. Therefore, different approaches have been used to improve its conductance through mixing with other conducting materials that may

enhance its electrochemical performance. For example, mixing GO with MWCNTs showed completely new characteristics (Li et al. 2013). In another note, Pyrogallol (PG) has three hydroxyl groups and used as an electro-catalytic reagent and mediator for the determination of many analytes (Attia et al. 2015; Ensafi et al. 2010).

Optimization using traditional approaches such as "one variable-at-a-time" usually extracts less information about variables beside being time and effort consuming (Regiart et al. 2015). Alternatively, experimentally designed optimization is a rational approach to extract more information with least number of experiments, thus time and cost effective. Central composite design (CCD) is one of the important experimental designs that is useful in extracting main and quadratic terms along with the possible interactions between studied variables.

Herein, we are making use of the advantages of all of the above mentioned materials and methods. We report on the electrochemical determination of OME using MWCNTs/GO/PG modified electrode that has not been reported before, making advantage of the factorial design as well as the properties of MWCNTs, GO and PG. Our sensor provides a new attempt for further enhancement of the electroanalytical potential of the OME configuration.

2. Experimental

2.1. Materials and reagents

OME was kindly supplied from Novartis Pharmaceutical Co., Egypt, with purity of 99.12%; 5-hydroxyomeprazole and omeprazole sulphone and were purchased from Sigma; Omez 20® (each tablet contains 20 mg OME, Pharos Pharmaceuticals). Britton-Robinson buffer (B-R buffer) 4.0 x 10^{-2} M was prepared by mixing H_3PO_4, acetic acid and boric acid with the appropriate amount of 0.2 M NaOH to obtain the desired pH (2.0 –10.0). Fresh human serum was obtained from the blood bank (VACSERA, Cairo, Egypt). Pyrogallol was purchased from Alpha Chemika, Mumbai, India. Pure graphite powder was obtained from Aldrich. Multiwalled carbon nanotubes (MWCNTs; 30 ± 15 nm diameter, 5–20 μm length, purity > 95%, was obtained from NanoLab (Waltham, MA, USA).Paraffin oil from Merck was used as the pasting liquid for the preparation of the paste electrodes.

2.2. Instruments and experimental conditions

Voltammetric measurements were carried out using CHI 760A Electrochemical Workstation (CH Instrument Inc., USA). A platinum wire (BAS, USA) was employed as the auxiliary electrode. All the cell potentials were measured with respect to Ag/AgCl (3.0 M NaCl) reference electrode (BAS, USA). All the electrochemical experiments were performed at ambient temperature of 25±1^{o}C.

Scanning electron microscopy (SEM) measurements were carried out using a Zeiss SEM Ultra 60 field emission scanning electron microscope (FESEM). The crystalline phases were detected and identified using an X-ray diffractometer (XRD) on an X'Pert PRO MRD with a copper source at a scan rate (2θ) of 1^{o}s^{-1}. Statistical interpretations were carried out using JMP® Copyright © 2012, SAS Institute Inc., Cary, North Carolina, USA.

2.3. Preparation of different electrodes

Carbon paste unmodified electrode (CPE) was prepared by mixing graphite powder (0.5 g) with paraffin oil (0.3 mL) in a glassy mortar. The carbon paste was packed into the hole of the electrode body and smoothed on a filter paper until it has its shiny appearance. In order to prepare MWCNTs/GO/PG modified electrode, first GO was prepared by Hummer's method(Hummers Jr and Offeman 1958) then MWCNTs were dispersed with GO in water (Aboutalebi et al. 2011) by adding 25 mg MWCNTs and 25 mg GO in 50 ml volumetric flask (1:1, w:w%) and sonicated for 45 min to produce a homogeneous dispersion. The formed MWCNTs/GO nanocomposite was centrifuged at 3000 rpm to remove the loosely bound MWCNTs and washed several times with water. The purified MWCNTs/GO composite was then dried overnight. Finally, three different amounts of MWCNTs/GO nanocomposite (5, 10 and 15 mg) were separately mixed well with equivalent amounts of PG present in 1 g graphite. Each MWCNTs/GO/PG paste was mixed well with an appropriate amount of paraffin oil (0.25 mL) for 40 min until a uniform and homogeneous wetted paste was obtained. These pastes were packed into the hole of the electrode body and smoothed on a filter paper until shiny appearance. A new surface was obtained by pushing excess of the paste out of the syringe and polished with weighing paper.

2.4. Recommended Experimental procedure

MWCNTs/GO/PG was cycled between 500 -1430 mV with a scan rate of 100 mV s^{-1} in 4.0x10^{-2} M B-R buffer solution of pH 7.0 several times until a reproducible response was achieved. Following this, the modified MWCNTs/GO/PG was transferred into another cell containing 4.0x10^{-2} M Britton– Robinson buffer of pH 7.0 and the proper amount of OME. Cyclic voltammogrames were recorded between 400 -1100 mV with a scan rate of 100 mV s^{-1}. DPVs procedure, Aliquots equivalent to 2.0x10^{-10} M-1.0×10^{-4} M OME were transferred into a series of 5-mL volumetric flasks using micro pipette. The volume was completed to the mark with B-R buffer pH 7.0. Solutions were accurately transferred to the electrolytic cell and DPVs was recorded. The peak current at MWCNTs/GO/PG were measured at scan rate of 10 mVs^{-1} using DPVs method.

2.5. Analysis of real samples

Six capsules of Omez 20®(each tablet contains 20 mg OME, Pharos Pharma For Pharmaceuticals) were mixed and weighed, and the average mass per tablet was determined, and then dissolved in 50 mL methanol and sonicated for 60 min. Then, the solution was filtered into a 25.0 mL volume calibrated flask, and the residue was washed three times with methanol added to the flask and then diluted to the mark with the same solvent.

To prepare the spiked samples, serum samples were taken from a healthy individuals immediately prior to experiments. Ten microliters of supernatant was transferred quantitatively to a 5 mL volumetric flask spiked with different volumes of OME standard solution (1.0 mM) in B-R buffer solution of pH 7.0. The solution was transferred into the voltammetric cell to be analyzed without any further pretreatment.

3. Results and discussion

3.1. Surface characterization of the fabricated electrodes

Figure 1 shows FESEM images of the fabricated electrodes. The surface of the CPE is dominated with uniform and smooth shaped graphite flakes and separated layers, Figure 1A. Figure 1B shows the formation of fairly homogeneous GO structures with an average length of 261 nm. However, the SEM image of the MWCNTs/GO/PG is totally different, Figure 1C, where PG is uniformly distributed in the MWCNTs/GO matrix and covering the surface of the MWCNTs, resulting in the formation of homogenous, porous network structure. Note that the MWCNTs network can still be seen in Figure 1C, which endows the nanocomposite with

improved compatibility and exhibit random coiled and curved features due to the intrinsic Van der Waals attractions between the individual nanotubes as well as the large surface area. The formation of homogeneous nanocomposite implies that MWCNTs and PG have been regularly incorporated with GO/CPE. The SEM proves that GO and PG molecules were attached on the surface of MWCNTs. Comparing the EDX spectra of CPE, GO and MWCNTs/GO/PG reveals the presence of low density peak for oxygen in case of bare unmodified graphite CPE. In case of GO, the oxygen peak increases to about 63%, indicating complete oxidation of graphite into GO. For the MWCNTs/GO/PG nanocomposite, the intensity of the oxygen peak increases compared to that of bare CPE, which can be attributed to the presence of GO, MWCNTs and PG.

The crystal structure of the synthesized materials was investigated by XRD. The XRD pattern of GO showed a typical (002) GO peak at $2\theta = 10^{o}$, Figure 1D. On the other hand, graphite flakes exhibit a strong and sharp peak at 26.26^{o}, indicating highly ordered structure (Bykkam et al. 2013). The FT-IR spectrum of the GO confirms the successful oxidation of graphite, Figure 1E. Also, the broad and wide peaks appeared at 3439 and 1719 cm^{-1} are attributed to the oxygen-containing functional groups on graphite oxide (Tang et al. 2009), confirming the presence of different types of oxygen functionalities in GO (Zhang et al. 2009). While the absorption band at 1560 cm^{-1} can be ascribed to benzene rings (Si and Samulski 2008), the sharp intense peak at 1419 cm^{-1} can be attributed to CO-carboxylic.

The electroactive area of the electrode was obtained by the cyclic voltammetric method using 1.0 mM $K_3Fe(CN)_6$ in 0.1 M KCl at different scan rates, using the Randles-Ševčík equation for a quasi-reversible process (Compton and Banks 2007):

$$I_P = 2.65 \times 10^5 n^{\frac{3}{2}} A D^{\frac{1}{2}} C v^{\frac{1}{2}} \quad (1)$$

where I_p is the peak current, n is the number of electrons transferred in the electrochemical process, A is the electrode area, D is the diffusion coefficient, C is the redox probe concentration and v is the applied voltammetric scan rate. The used D value was 7.6×10^{-6} cm^2 s^{-1}. The electroactive area was calculated from the slope of the plot of I_p *versus* $v^{1/2}$. The calculated areas were 0.092 and 0.120 cm^2 for CPE and MWCNTs/GO/PG, respectively.

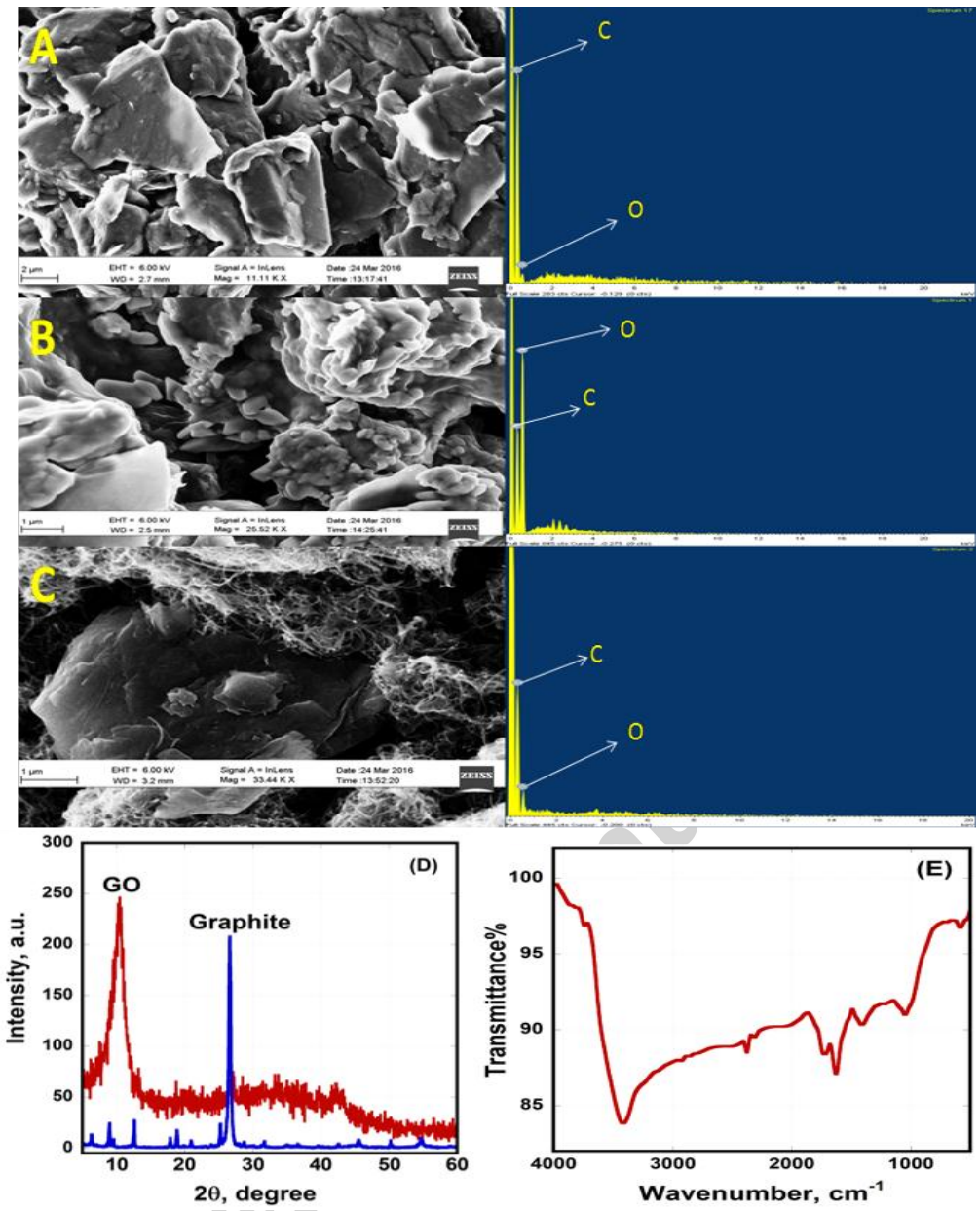

Figure 1: FESEM images of (A) CPE, (B) GO and (C) MWCNTs/GO/PG with their corssponding EDX spectra. The (D) XRD, and (E) IR spectra of GO.

3.2. Electrochemical Behavior of OME on different electrodes

The CPE, MWCNTs/CPE, MWCNTs/GO, and MWCNTs/GO/PG electrodes were tested towards the electrochemical sensing of OME, Figure 2A. Note that the optimal response was obtained using the MWCNTs/GO/PG-based sensor. In the absence of OME, no measurable anodic or cathodic peak currents were observed in the studied potential range indicating that the MWCNTs/GO/PG sensor has no

electroactivity in the selected potential range. In case of bare-unmodified CPE, the anodic peak current corresponding to the electrochemical oxidation of OME was observed. As depicted in Figure 2A, the magnitude of the voltammetric response of the sensor increases due to the synergistic effect of MWCNTs, GO and PG, indicating the possibility to use this composite for effective determination of OME. The results demonstrate the electrocatalytic efficiency of the four tested electrodes in the following order: MWCNTs/GO/PG > MWCNTs/GO/CPE > MWCNTs/CPE > CPE.

Electrochemical impedance spectroscopy (EIS) is one of the most powerful techniques for the convenient determination of both kinetic and mass-transport parameters as well as the charge transfer coefficient. Figure 2B shows the EIS response for CPE, MWCNTs/CPE, MWCNTs/GO/CPE and MWCNTs/GO/PG. EIS measurements were performed in 1.0 mM $K_3Fe(CN)_6$ (1:1) solution in 0.1 M KCl. The equivalent circuit model (inset of Figure 2B) was chosen to fit the obtained impedance data for the electron transfer process (modelled as a resistance to charge transfer, R_{CT}) and the diffusion process (modelled as the Warburg-type impedance, W). The R_{CT} and W were both in parallel with the interfacial capacitance (C). By fitting the data, R_{CT} was estimated to be 1823 Ω at the bare CPE, while it decreased to 1200 and 980 Ω for MWCNTs/CPE and MWCNTs/GO, respectively, and then decreased to 310 Ω for MWCNTs/GO/PG, indicating the significantly lower electron-transfer resistance of MWCNTs/GO/PG compared with other electrodes. The results are consistent with the CV results, demonstrating that the MWCNTs/GO/PG composite might provide higher electron conduction pathways due to the synergistic effects of its constituents.

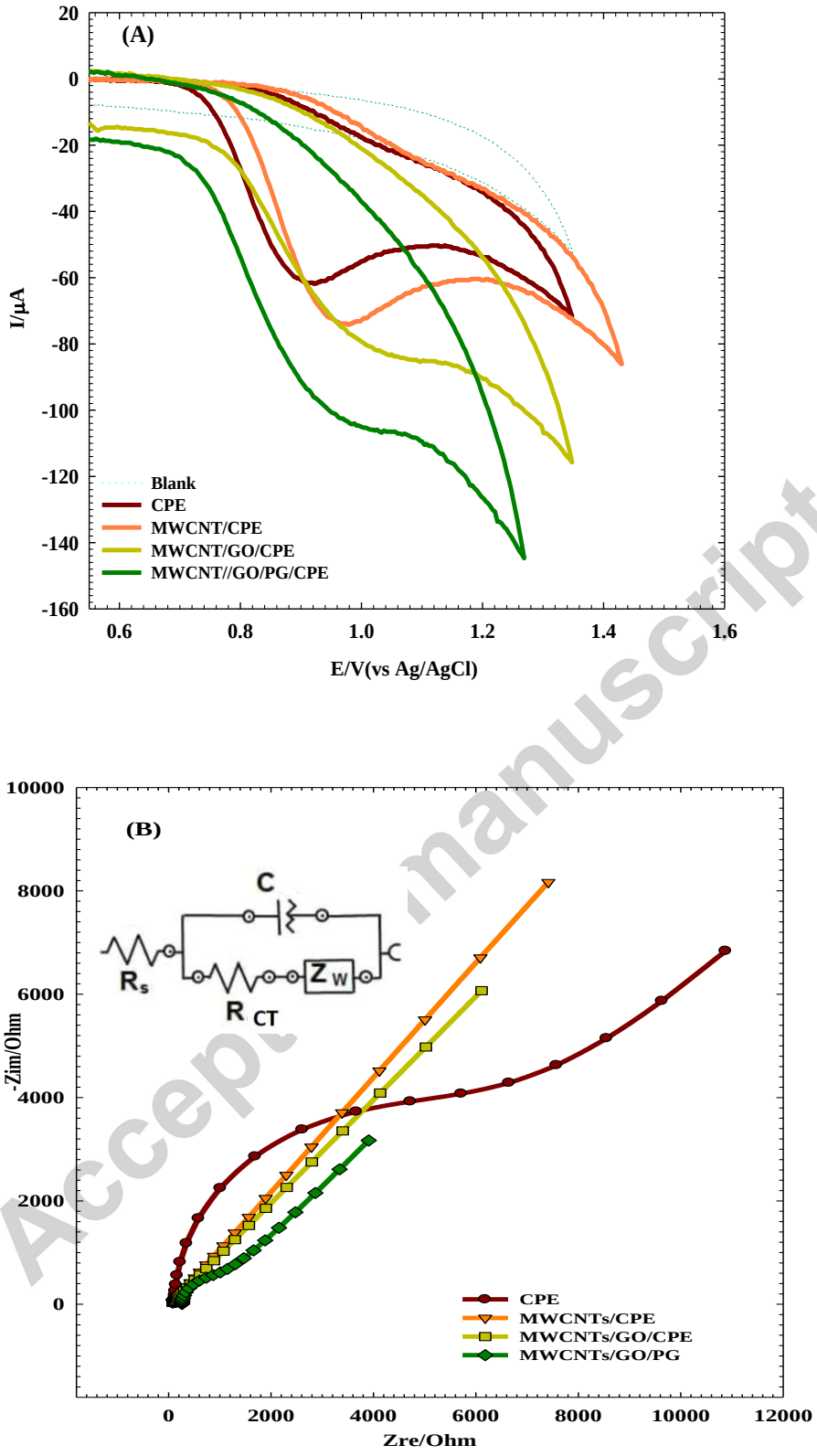

Figure 2: (A) Cyclic voltammogrames of 1.0 mM OME in B–R buffer (pH 7.0) at a scan rate of 100 mV s^{-1} recorded at CPE, MWCNTs/CPE, MWCNTs/GO/CPE and MWCNTs/GO/PG electrodes. **(B)** The impedance plots for CPE, MWCNTs/CPE, MWCNTs/GO/CPE and MWCNTs/GO/PG electrodes in 1.0 mM $K_3Fe(CN)_6$ (1:1) solution in 0.1 M KCl.

3.3. Effect of pH

Upon increasing the pH, the peak potential shifts towards less positive values, suggesting protonation-deprotonation process of OME. Analysis of the voltammetric response, in terms of the peak potential (E_p), shows a linear relationship with the pH of the buffer solution: $E_p(V)$ = 1.139-0.0582 *pH*, (R^2=0.9984), with the slope equals to the anticipated Nernstian value for a two–electron, two–proton electrochemical reaction. Note that the highest oxidation peak current was obtained at pH 7.0 (very close to the physiological pH).

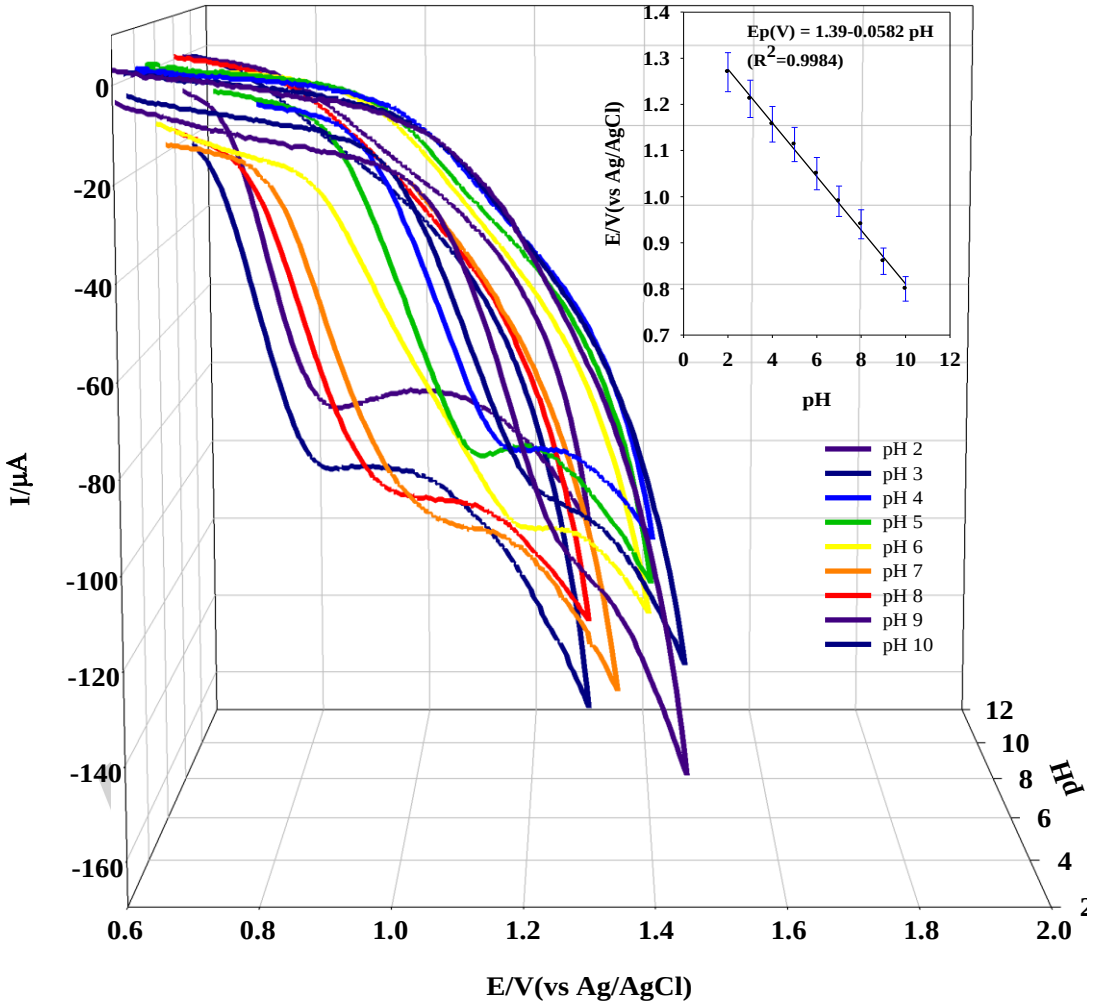

Figure 3: Cyclic voltammetric response of 1.0 mM OME at different pH values using MWCNTs/GO/PG; scan rate of 100 mV s^{-1}. The inset: plot of anodic peak potential of OME *versus* pH.

3.4. Effect of scan rate

The influence of scan rate (v), in the range of 10 to 100 mV s^{-1}, on the electrochemical response of MWCNTs/GO/PG in 1.0 mM OME was studied, see Figure S1 in the ESI. A linear relationship (I_p (μA) = -35.59+11.33$v^{1/2}$ (V s^{-1})$^{1/2}$, R^2= 0.9922) was observed between the peak current (I_{pa}) and square root of the scan rate ($v^{1/2}$), suggesting that the process is diffusion-controlled. Furthermore, it was noticed that the oxidation peak potential (E_p) was also scan rate dependent, where increasing the scan rate resulting in a shift to more positive potentials, see inset B in Figure S1. The linear relationship between E_p and log v can be described by the regression equation *$y=147.5a+729.98$, $R^2=0.9979$.*

The linear relationship between E_p and log v can be described via the regression equation *$y=147.5a+729.98$, $R^2=0.9979$.* According to Laviron (Laviron 1979), for an irreversible electrode process, E_{pa} is defined as:

$$E_{pa}= E^{o'}+ \frac{2.303RT}{\alpha nF} log \frac{RTk^o}{\alpha nF} logv \qquad (2)$$

where α is the charge transfer coefficient, k^o is the standard heterogeneous rate constant, n is the number of electrons transferred, v is the scan rate, $E^{o'}$ is the formal redox potential, and other symbols have their usual meanings. According to Bard and Faulkner (Bard and Faulkner 1980), α can be given as:

$$\alpha= \frac{47.7}{E_{p-E_{p/2}}} mV \qquad (3)$$

where $E_{p/2}$ is the potential at which the current is at half peak value. The resulting electrochemical parameters of OME on the MWCNTs/GO/PG are: αn=0.74, α=0.37, $E^{o'}$=0.882 and k^o=110.15 s^{-1}. The number of transferred electrons (n) was calculated and found to be 2. Additionally, this consideration can be confirmed by calculating the surface concentration (Γ) of compounds adsorbed onto MWCNTs/GO/PG surface (Bard and Faulkner 1980). The surface concentrations (Γ) were determined via:

$$I_{pa}=\frac{n^2F^2 \nu A\Gamma}{4RT} \qquad (4)$$

where n is the number of electrons, F is the Faraday's constant, ν is the scan rate, A is the active area, Γ is the surface concentration of electroactive species, R=8.314 J mol^{-1} K^{-1} and T = 298 K. Γ values were found to be 1.02 x 10^{-6} and 7.63 x 10^{-6} mol cm^{-2}

for CPE and MWCNTs/GO/PG, respectively, confirming the higher affinity and interaction of modifiers towards the OME oxidation, showing the synergistic effect of MWCNTs, GO and PG in improving the detectability of OME.

3.5. Chronoamperometry

Figure S2 shows the chronoamperometric measurements of OME, performed at a constant potential (1035 $mV_{Ag/AgCl}$) in B-R buffer (pH 7.0).

Using Cottrell's law (Bard and Faulkner 1980), the diffusion coefficient D can be calculated. According to the Cottrell equation, the slope obtained from the relation between anodic peak current and $t^{-1/2}$ (inset) equals $nFA(D/\pi t)^{1/2}$, so D of OME was calculated to be 5.28×10^{-5} cm^2 s^{-1} [See Supplementary material (Figure 2 inset)] shows the calibration curve as a linear relationship between different OME concentrations and the current at a fixed time.

3.1. Optimization of DPVs

Owing to the fact that more than one variable is highly important, and that it would be difficult to optimize the conditions through one variable at a time, the studied factors were experimentally designed. One of the main aims of experimental methodologies is to find the optimal level for each studied variable by doing the least number of experiments. Based on the preliminary experiments, the highest and lowest values of each variable were defined to be 10-30 mg for modifier concentration, 5–9 for pH and 10 - 20 mV/sec for the scan rate.

Two-level factorial design is very useful for preliminary studies or in the initial optimization step due to their simplicity and relatively low cost.

For this design, 16 experiments were necessary, which were realized in triplicate and randomized to eliminate any uncontrollable or extraneous conditions.

The critical terms to be included in the model for subsequent data analysis and optimization were initially screened. Half normal plot (Figure 4A) showed that all main effects are significant, besides the significant effects of Modifiers% and pH quadratic terms. These linear and quadratic terms should be included in our model in order to optimize all the studied factors that affect our objective response. Afterwards,

the above-mentioned variables were optimized by the response surface methodology, where the polynomial equation can be expressed as:

$$Y=50.76 - 2.66\ X_1+1.69\ X_2-0.55\ X_3+0.24\ X_1^2-2.25\ X_2^2 \quad (5)$$

where Y is the current (response), X_1 is the Modifier% factor, X_2 is the pH factor and X_3 is the scan rate factor. The coefficient of determination (R^2) of the model was 0.940 and root mean square error (RMSE) was 2.982, indicating adequate fit of the prediction model. The magnitude of factors' effect can be evaluated based on their corresponding coefficients in the last equation. Obviously, the linear terms of pH and modifier% have larger effect with respect to scan rate. Changing modifier% from low to high levels has a negative effect on the response, whereas positive response would result upon changing pH from low to high levels. Opposite effect was observed for the quadratic terms compared to the main effects of modifiers% and pH. At extreme levels (high and low) of modifiers% or pH, the response would increase or decrease, respectively. This also can be concluded from the curvature of the surface plot (Figure 4B). The statistical analysis of coefficients revealed that all studied linear and quadratic terms have significant effect on the peak current at p 0.05. It is worth noting that the effect of pH quadratic term is more pronounced than its main effect. On contrary, the main effect of modifier% is noticeable. Pareto chart (Figure 4C) was used to visualize the estimated effect of variables. The bar lengths are proportional to the absolute values of estimated effects and the vertical reference line indicates a t-value of 2.446 at a confidence level of 95.0%. The chart showed that the variables were considered as statistically significant factors. Furthermore, all the previous observations have been substantiated.

It can be proven that the studied factors are significant. According to desirability function in JMP®, the maximum response could be achieved using 10 mg modifiers (5 mg GO/MWCNTs + 5 mg PG) at pH 7.0 with a scan rate of 10 mV/sec. It can be observed in the surface shape that the optimal region was found and also that the maximum response was achieved when the pH was 7, SR was 10 and modifiers concentration was 10 mg.

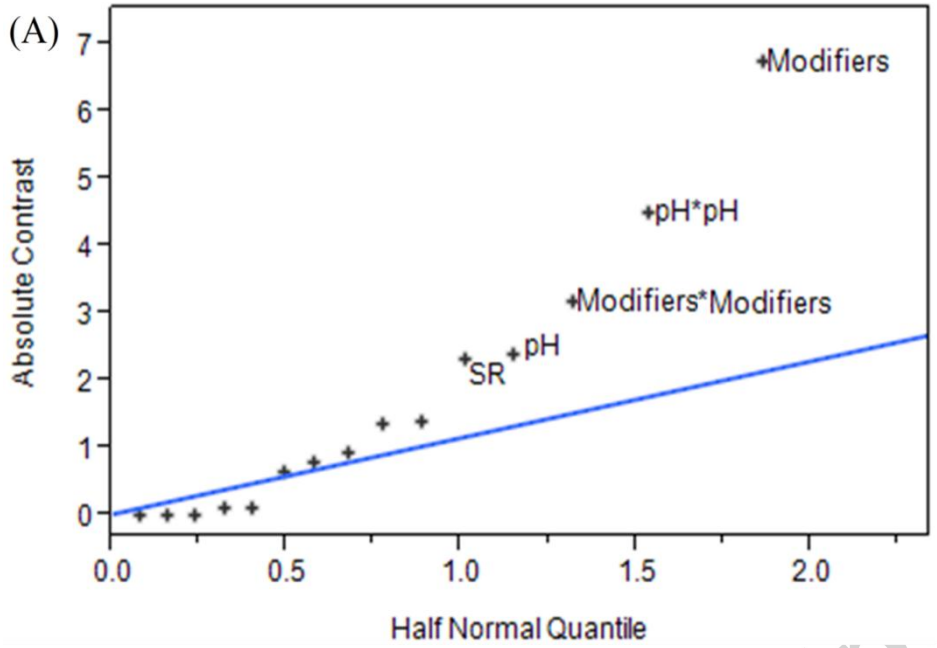

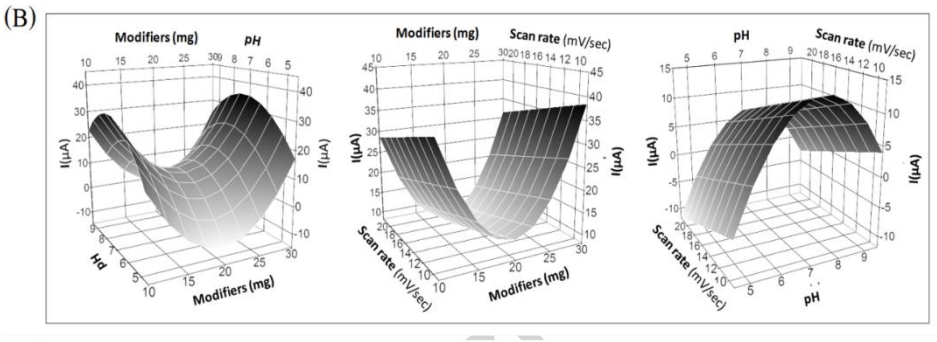

(C) **Sorted Parameter Estimates**

Term	Estimate	Std Error	t Ratio	Prob>|t|
Modifiers	-2.6625	0.389776	-6.83	<.0001*
(pH)*(pH)	-2.25	0.372768	-6.04	0.0001*
Modifiers *Modifiers	0.238	0.05595	4.25	0.0017*
pH	1.6875	0.527174	3.20	0.0095*
SR	-0.554545	0.17983	-3.08	0.0116*

Figure 4: (A) Half normal plot showing the absolute value of the contrasts against the normal quantiles for the absolute value normal distribution, (B) response surface plots for the main effects of studied factors on the current and (C) the standardized main effect Pareto chart for the studied main and quadratic terms.

3.7. Analytical characterization and method validation

The optimized conditions for OME determination *via* DPVs (pH 7.0, SR 10 and 10 mg of the modifiers) were used. The guidelines provided by the International Conference on Harmonization (ICH)(Guideline 1997) for methods validation were followed for the validation of our suggested method. DPVs experiments were

performed using MWCNTs/GO/PG in B-R buffer pH 7.0 solution containing various individual concentrations of OME. The calibration range was established through consideration of the necessary practical range, according to OME concentration present in the pharmaceutical product, to give accurate, precise and linear results, Figure 5. The plot of the peak current *vs.* OME concentration showed two linear segments with different slopes for the OME concentrations: for 2.0×10^{-10}– 6.0×10^{-6} M, the regression equation was I(μA)=0.322 C + 1.311 (R^2=0.9991), while for 6.0×10^{-6} – 1.0×10^{-4} M, the regression equation was I(μA)=0.0293 C + 3.748 (R^2=0.9993). The decrease in sensitivity (slope) of the second linear segment is likely due to kinetic limitations (K Gupta et al. 2011).

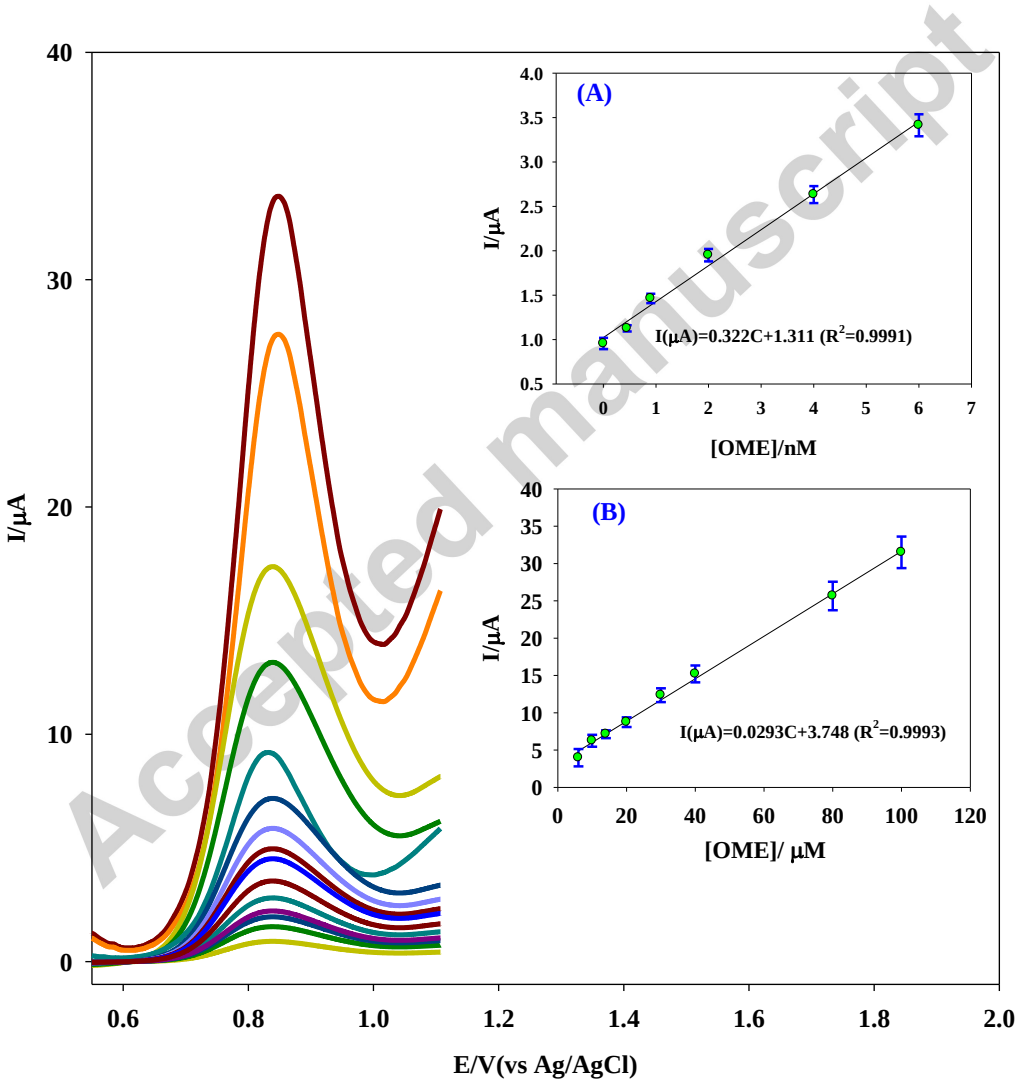

Figure 5: DPVs of OME in B–R buffer solution (pH 7.0) containing different concentrations of OME at a scan rate of 10 mV s^{-1}. Insets: the plot of the peak current as a function of OME in the concentration range (A) 2.0×10^{-10}– 6.0×10^{-6} M, and (B) 6.0×10^{-6}–1.0×10^{-4} M.

The limit of detection (LOD) was found to be 1.02×10^{-11} M. The limit of quantification (LOQ) was found to be 3.41×10^{-11} M. The intraday and interday precisions were in the range 0.88–1.15% and 0.87–1.08%, respectively. The peak current does not change after storage in air for 8 days. The modified electrode retained 99.01% of its initial response up to one month.

The influence of various species that potentially interfere with the determination of the studied drug was investigated under optimum conditions using 1.0 mM at pH 7.0. The proposed sensor was tested for the voltammetric analysis of OME in the presence of the frequently co-formulated drugs tinidazole and doxycycline. However, MWCNTs/GO/PG showed high specificity to OME, because tinidazole and doxycycline have no peak at this material in the studied range. Another species were chosen from a group of substances that are commonly found in pharmaceutical preparations, such as lactose, starch, glucose, cellulose, sucrose, crosscarmellose sodium, colloidal silicon dioxide and magnesium stearate. According to the results, the substances showed no interference, as the tolerance limit was less than ±5% of OME. For biological application, the electrochemical responses of 5-hydroxyomeprazole and omeprazole sulphone as the main two metabolites of OME present in serum were tested. The sensor showed sufficient selectivity to OME in presence of metabolites since no electrochemical response was observed while testing these metabolites.

Our work provides a simple and cheap sensor that has merits over prior art with a large linear range, which is applicable for sensing drugs in pharmaceutical and biological applications. To put this into context, the analytical parameters for the proposed modified electrode presented in the present study are comparable with reported values in literature for the detection of OME, with the advantage of providing wider range with optimized procedures and lower detection limits than other reported electrochemical methods, with lower prediction error, Table S1.

3.8. Analytical application

MWCNTs/GO/PG sensor was successfully applied to the determination of OME tablet and human serum samples. Mean recovery results and the relative standard deviation are given in Table S2. According to the recovery results, a good accuracy and precision were found for the analysis of Omez20® by the newly

developed sensor. The calibration curve of OME in serum showed a straight line in the linear dynamic range (2.0×10^{-7} M – 2.0×10^{-4} M) with the regression equation I(μA)=0.0285C+0.818 (R^2=0.9992), the LOD is 1.11 $\times10^{-8}$ M and the LOQ is 3.69 $\times10^{-8}$ M. OME was determined after the addition to the human serum samples, and the recovery values were calculated. The results are given in Table S3, where the recovery values were between 98.00 and 101.10 %, showing very satisfactory results. Statistical calculations were made in order to check the confidence and correlation between the suggested procedures and the reported method. From the calculated t– and F–values at the 95% confidence level, it is clear that the results obtained by the developed method is in good agreement with those of standard method (British Pharmacopoeia 2003), see Table S3.

Evidently, sample pre-treatment always precedes the reported liquid chromatographic methods for OME biological applications. An exceptional micellar chromatographic method was reported for OME analysis in serum samples without pre-treatment but filtration (Rambla-Alegre et al. 2009). Not only did the sensor lower the detection limit reasonably but the sensor also considered as a green analytical method. The proposed method fulfil the green analytical principles (Gałuszka et al. 2013) where the sensor can determine OME in a small sample volume without derivatization. In situ measurements were carried out directly in serum samples without any treatment or even filtration. The miniaturized sensor saves energy, reduces solvent consumption and produces minimal waste. Finally, with the aid of chemometrics, the proposed sensor is considered to be multi-analyte method.

4. Conclusions

Incorporation of MWCNTs, GO and PG as modifying species in carbon paste electrode was evidenced to enhance the electrochemical response towards OME. Experiment design was used to improve OME determination with a desirability function criteria that successfully optimize the levels of instrumental and non-instrumental factors. The electrochemical behavior of OME was studied by cyclic voltammetry. The low detection limit, the ease of preparation and regeneration of the electrode surface, as well as the long time stability and reproducibility, make the system very useful in the construction of simple devices for the determination of OME in the presence of many interfering species and in pharmaceutical and biological samples.

Refrences

Aboutalebi, S.H., Chidembo, A.T., Salari, M., Konstantinov, K., Wexler, D., Liu, H.K., Dou, S.X., 2011. Energy Environ. Sci. 4 (5), 1855-1865.

Attia, A.K., Salem, W.M., Mohamed, M.A., 2015. Acta Chim. Slov. 62 (3), 588-594.

Banks, C.E., Davies, T.J., Wildgoose, G.G., Compton, R.G., 2005. Chem. Commun. 7, 829-841.

Bard, A.J., Faulkner, L.R., 1980. Electrochemical methods: fundamentals and applications. Wiley New York.

Bosch, M.E., Sánchez, A.R., Rojas, F.S., Ojeda, C.B., 2007. J. Pharm. and Biom. Analysis 44(4), 831-844.

British Pharmacopoeia, 2003. Her Majestyís Stationery Office. London.

Bykkam, S., Rao, K., Chakra, C., Thunugunta, T., 2013. Synthesis and characterization of graphene oxide and its antimicrobial activity against klebseilla and staphylococus. Int. J. Adv. Biotechnol. Res 4(1), 142.

Compton, R.G., Banks, C.E., 2007. Understanding voltammetry. World Scientific.

Ensafi, A.A., Arabzadeh, A., Karimi-Maleh, H., 2010. Anal. Lett. 43(12), 1976-1988.

Gałuszka, A., Migaszewski, Z., Namieśnik, J., 2013. TrAC Trends Anal Chem. 50, 78-84.

Gao, C., Guo, Z., Liu, J.-H., Huang, X.-J., 2012. Nanoscale 4(6), 1948-1963.

Guidelines, I.C.H, 1997. Q2B validation of analytical procedures: methodology. Fed. Regist 62.

Hummers Jr, W.S., Offeman, R.E., 1958. J. Am. Chem. Soc. 80(6), 1339-1339.

K Gupta, V., Nayak, A., Agarwal, S., Singhal, B., 2011. Comb. Chem. High Throughput Screen 14(4), 284-302.

Laviron, E., 1979. J Electroanal Chem 101: 19. doi: 10.1016. S0022-0728 (79), 80075-80073.

Li, J., Kuang, D., Feng, Y., Zhang, F., Xu, Z., Liu, M., Wang, D., 2013. Microchimica Acta 180(1-2), 49-58.

Mohamed, M.A., Abdelwahab, N.S., Banks, C.E., 2016. Anal. Methods 8(22), 4345-4353.

Olbe, L., Carlsson, E., Lindberg, P., 2003. Nat. Rev. Drug Discov. 2(2), 132-139.

Rambla-Alegre, M., Esteve-Romero, J., Carda-Broch, S., 2009. Analytica chimica acta 633(2), 250-256.

Regiart, M., Escudero, L.A., Aranda, P., Martinez, N.A., Bertolino, F.A., Raba, J., 2015. Talanta 135, 138-144.

Si, Y., Samulski, E.T., 2008. Nano letters 8(6), 1679-1682.

Stankovich, S., Dikin, D.A., Piner, R.D., Kohlhaas, K.A., Kleinhammes, A., Jia, Y., Wu, Y., Nguyen, S.T., Ruoff, R.S., 2007. Carbon 45(7), 1558-1565.

Tang, L., Wang, Y., Li, Y., Feng, H., Lu, J., Li, J., 2009. Adv. Funct. Mater. 19(17), 2782-2789.

Wang, Y., Li, Y., Tang, L., Lu, J., Li, J., 2009. Electrochem. Commun. 11(4), 889-892.

Zhang, T., Zhang, D., Shen, M., 2009. Mater. Lett. 63(23), 2051-2054.

Highlights

- A novel electrochemical sensor was constructed and tested.
- The sensor was used for the determination of omeprazole in real samples.
- Modification improved the sensitivity and detection limit of the sensor.
- The developed method was optimized using central composite design.
- The sensor showed the lowest detection limit so far.